# The adaptive architecture is shaped by population ancestry and not by selection regime

**Kathrin A. Otte[1,#], Viola Nolte[1,#], François Mallard[1,2], Christian Schlötterer[1,*]**

[1]*Institut für Populationsgenetik, Vetmeduni Vienna, Vienna, Austria*

[2]*Present address: Institut de Biologie de l'École Normale Supérieure, CNRS UMR 8197, Inserm U1024, PSL Research University, F-75005 Paris*

[#]both authors contributed equally

[*]corresponding author: christian.schloetterer@vetmeduni.ac.at

**Key words:** Experimental Evolution, Temperature Adaptation, Adaptive Architecture

**Abstract**

**Understanding the genetic architecture of adaptive phenotypes is a key question in evolutionary biology. One particularly promising approach is Evolve and Resequence (E&R), which combines advantages of experimental evolution such as time series, replicate populations and controlled environmental conditions, with whole genome sequencing. The recent analysis of replicate populations from two different *Drosophila simulans* founder populations, which were adapting to the same novel hot environment, uncovered very different architectures - either many selection targets with large heterogeneity among replicates or fewer selection targets with a consistent response among replicates. Here, we exposed the founder population from Portugal to a cold temperature regime. Although almost no selection targets were shared between the hot and cold selection regime, the adaptive architecture was similar: we identified a moderate number of loci under strong selection (19 selected alleles, mean selection coefficient = 0.072) and very parallel responses in the cold evolved replicates. This similarity across different environments indicates that the adaptive architecture depends more on the ancestry of the founder population than the specific selection regime. These observations have a pronounced impact on our understanding of adaptation in natural populations.**

## Introduction

Adaptation of natural populations to environmental change may either occur from standing genetic variation or by the acquisition of new mutations. The relative importance of these two paths crucially depends on the underlying adaptive architecture (Barghi et al. 2020) of the focal trait. The adaptive architecture differs from the genetic architecture, which is inferred by QTL mapping and GWAS, by accounting for pleiotropic constraints as well as for the large body of deleterious mutations (Gazal et al. 2017; Zeng et al. 2018). Depending on the context, two different aspects of the adaptive architecture are emphasized. The focus is either the identity of specific loci/SNPs or the general characteristics of the adaptive architecture characterized by the number of contributing loci and their effect sizes and frequency in the focal population (Barghi et al. 2020).

Contributing loci are either identified by QTL/GWAS studies (Flint and Mott 2001; McCarthy et al. 2008) or with genomic selection scans, which apply statistical tests to detect selection signatures from population polymorphism data (Storz 2005; Vitti et al. 2013). Some selection scans assume that selection targets are shared among populations exposed to the same environment, because such parallel signatures provide additional statistical support (Turner et al. 2010; Lee and Coop 2017; Harris and DeGiorgio 2020). Many selection targets were successfully identified with these strategies and have contributed to our understanding of the molecular basis of adaptation processes (e.g. Turner et al. 2010; Jones et al. 2012; Roesti et al. 2014; Reid et al. 2016; Johnson and Voight 2018). It is, nevertheless, not apparent to what extent these results can be generalized, because most adaptive traits have a polygenic basis (Barton and Keightley 2002; Sella and Barton 2019) and either only small allele frequency changes (Sella and Barton 2019) or non-parallel responses are expected (Barghi et al. 2020).

The key concept of polygenic adaptation is that multiple loci are contributing to the phenotype, and rather than focusing on particular loci, the collective effect of all loci needs to be considered to estimate the phenotypic value of a given trait. This has important implications for the understanding of the adaptive architecture (Barghi et al. 2020).

The infinitesimal model (Fisher 1918; Bulmer 1971; Barton et al. 2017) is the most extreme case of polygenic adaptation and is frequently approximated by very many contributing loci, each of

very small effect. When many loci are contributing to a phenotype under stabilizing selection, any selection regime changing the trait optimum will result only in very small allele frequency shifts (Bulmer 1971; Sella and Barton 2019) - almost impossible to detect with classic population genetic tests (Pritchard et al. 2010; Field et al. 2016; Jain and Stephan 2017a).

Even when these conditions are relaxed and a distribution of effect sizes with some large effect alleles is considered, no pronounced allele frequency changes are expected when the populations are large and in mutation selection equilibrium: alleles with large effects are segregating at low frequencies only and do not contribute much to the phenotypic variance of the population upon which selection is operating (de Vladar and Barton 2014; Jain and Stephan 2017b). Theory predicts that as the pool of contributing loci to the selected phenotype becomes smaller (i.e. a decreased mutational target), larger allele frequency changes are expected that will progressively be detected in population genetic analyses (Höllinger et al. 2019). Therefore, traits with an intermediate number of contributing loci are particularly interesting, because the response of these loci can be sufficiently strong to be detected in experiments while, at the same time, being informative about polygenic adaptation: more loci are segregating in the population than required to reach a new trait optimum (i.e. genetic redundancy).

The consequence of this genetic redundancy is that the contribution to the phenotype can be highly heterogeneous for individual loci in differentiated populations if they vary in frequency. This expectation nicely conforms with empirical data, mostly from QTL studies, which find heterogeneous sets of contributing loci among different populations (Adeyemo et al. 2009; Wu et al. 2013; Al Olama et al. 2014; Li and Keating 2014; Conte et al. 2015; Horikoshi et al. 2018; Takata et al. 2019; Wojcik et al. 2019; Zan and Carlborg 2019; Hodonsky et al. 2020). In the case of adaptation to a new trait optimum, genetically differentiated populations will adapt by frequency changes of different sets of loci. Hence, for polygenic adaptation the identity of individual selected loci is not very important to describe the adaptive architecture, rather information about the number of loci, effect sizes and frequencies are needed to understand the selective response.

Selection signatures not shared among natural populations are difficult to interpret, as the distinction between population-specific selection targets and false positive/negative signals can

be challenging given the high impact of a largely obscure demography on selection signatures (Jensen et al. 2005; Stajich and Hahn 2005; Li et al. 2012; Lohmueller 2014; Pavlidis and Alachiotis 2017; Johri et al. 2020). Experimental evolution, in contrast, provides the advantage of replicate populations, which evolve from the same founder population under controlled experimental conditions (Kawecki et al. 2012). The potential of experimental evolution to study the genomic signatures of polygenic adaptation has, however, not yet been fully exploited since most studies apply truncating selection. Thus, the contributing alleles experience continued selection pressure throughout the entire experiment, causing a parallel selection response in the replicate populations towards an extreme phenotype. Laboratory natural selection is a specific experimental evolution design, where the evolving populations are exposed to a new environment (Garland and Rose 2009). In contrast to truncating selection, populations are expected to reach a new phenotypic optimum. In combination with whole genome sequencing, it provides an interesting approach to study the adaptive architecture experimentally.

Two previous experimental evolution studies conducted in the same novel hot laboratory environment revealed very different adaptive architectures (Mallard et al. 2018; Barghi et al. 2019). In the Portugal experiment, five strongly selected genomic regions were identified and this selection signal was highly parallel across replicates. For the Florida experiment, 99 selection targets were identified and considerable heterogeneity was observed between the replicates. One possible explanation for this different adaptive architecture is that the ancestral trait optima differed between the two founder populations (Barghi and Schlötterer 2020), leading to a more intense selection in the Portugal experiment, because it was less well adapted than the Florida founder population to high temperatures. Alternatively, more large effect alleles may have been segregating at higher frequencies in the Portugal founder population.

Here, we exposed replicate populations of the Portugal founders to a cold temperature regime to shed more light on the different selection responses. Interestingly, we found very little overlap between the genomic position of the selection targets in the hot and cold temperature regimes. Most large effect loci detected in the hot environment did not respond in the cold, suggesting that hot and cold temperature adaptation may be different traits, rather than a simple shift in optimum of the trait ‘temperature adaptation’. Nevertheless, adaptation to both, hot and cold, temperature

105 regimes had a very similar adaptive architecture - with a comparable number of selection targets
106 and effect sizes. We conclude that the adaptive architecture differs between populations and may
107 be trait independent. We discuss to what extent this phenomenon can be explained by the
108 infinitesimal model.

109 **Results**

110 We studied the genetic architecture of cold adaptation in *Drosophila simulans* by combining
111 experimental evolution with whole genome re-sequencing (Evolve and Resequence, E&R). Five
112 replicate populations originating from the Portuguese founder population described by Mallard et
113 al. (2018) evolved for more than 50 generations (about four years) in a cold temperature regime
114 with daily fluctuations between 10°C and 20°C. Genome-wide allele frequencies were
115 determined in 10 generation intervals by sequencing pools of individuals (Pool-Seq (Schlötterer
116 et al. 2014)). Contrasting generation 0 with 51 we identified 6,527 SNPs, which changed in
117 frequency more than expected by genetic drift either across all five replicates (adapted CMH test
118 (Spitzer et al. 2020), 6,510 SNPs) or at least in one replicate (adapted $\chi^2$ test (Spitzer et al. 2020),
119 additional 17 SNPs). The X chromosome harbored only 142 SNPs. Such a low number of
120 candidate SNPs on this chromosome was not seen in other *Drosophila* E&R studies that
121 observed similar numbers of candidate SNPs on the X chromosome and autosomes (Jha et al.
122 2015; Jha et al. 2016; Barghi et al. 2019; Kelly and Hughes 2019; Michalak et al. 2019).
123 The pronounced peak structure in the Manhattan plot (Figure 1A) indicates that many candidate
124 SNPs are not independent due to linkage (Nuzhdin and Turner 2013; Franssen et al. 2017a). We
125 accounted for this and employed a correlation-based haplotype reconstruction approach to
126 identify independently selected haplotype blocks based on their distinct trajectories (Franssen et
127 al. 2017a; Otte and Schlötterer 2017) and treated each of these haplotype blocks as a single target
128 of selection (Barghi et al. 2019).

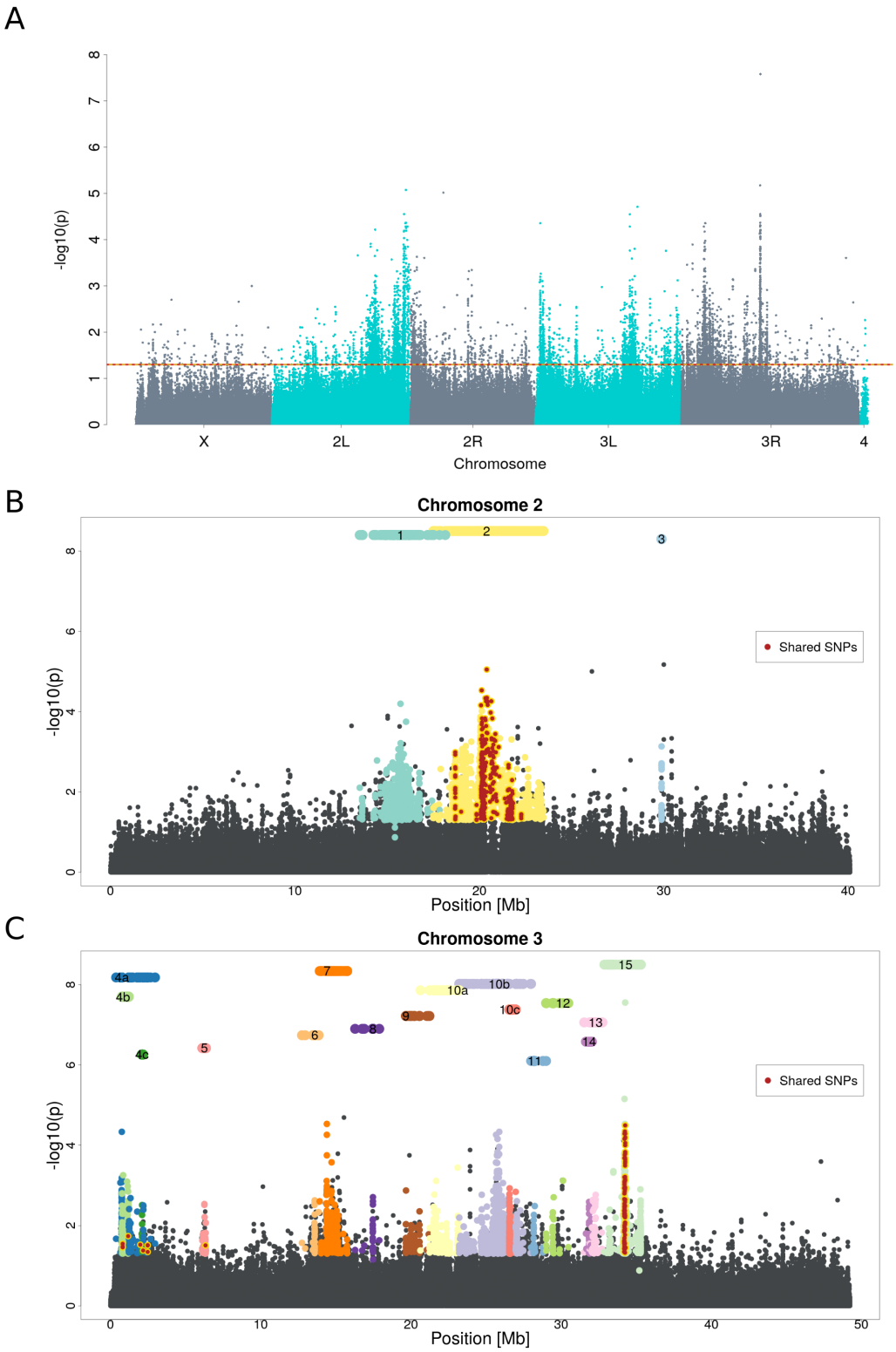
A
-log10(p)
0
1
2
3
4
5
6
7
8
X
2L
2R
3L
3R
4
Chromosome
B
Chromosome 2
1
2
3
Shared SNPs
-log10(p)
0
2
4
6
8
0
10
20
30
40
Position [Mb]
C
Chromosome 3
4a
4b
4c
5
6
7
8
9
10a
10b
10c
11
12
13
14
15
Shared SNPs
-log10(p)
0
2
4
6
8
0
10
20
30
40
50
Position [Mb]

129 Figure 1: Manhattan plots of the genomic selection signature in response to cold temperature.
130 A) p-values were obtained from an adapted CMH test (Spitzer et al. 2020) comparing the founder
131 generation (F0) to the most advanced (F51) generation. The dotted line indicates the significance
132 threshold (p-value < 0.05 after correction for multiple testing). B, C) A close up of the Manhattan plot in
133 panel A for chromosomes 2 and 3. Each selected haplotype block and the corresponding candidate SNPs
134 are shown in a distinct color. Numbered bars above the Manhattan plot indicate the position of the
135 selected haplotype blocks. Some blocks, which can be further subdivided by the analysis of earlier time
136 points, are labeled with letters (e.g. 10a, 10b etc.). SNPs with significant allele frequency changes in both,
137 hot and cold, selection regimes (shared SNPs) are colored in dark red.

138 Selected haplotype blocks in the cold-evolved *D. simulans* population

139 Because the small number of candidate SNPs precluded haplotype block reconstruction on the X
140 chromosome, all 15 haplotype blocks were identified on the major autosomes (Figure 1B, 1C).
141 The size of the haplotype blocks ranged from 5 kb to 6 Mb. Three of the 15 blocks were located
142 on chromosome 2 while all others fell on chromosome 3.
143 The 15 selected haplotype blocks were identified by clustering SNPs with similar allele
144 frequency trajectories in the five replicates and six time points. A conservative assumption is that
145 each of the selected haplotype blocks contains one selection target. Nevertheless, multiple
146 selection targets can recombine during the experiment onto a single haplotype block, which
147 outcompetes the individual parental haplotype blocks (Otte and Schlötterer 2019). Such
148 multiple-target haplotypes will dominate the later phases of the experiment and are considered as
149 a single selected haplotype. To identify such cases, we repeated the haplotype block
150 reconstruction with fewer generations - four time points up to generation 31 - and found that two
151 reconstructed haplotype blocks could be further broken up: block 4 and 10 were split into three
152 different blocks each (4a, 4b, 4c and 10a, 10b, 10c, see Figure 1C). This observation confirms
153 that the number of inferred independent haplotype blocks is a conservative estimate of the
154 number of selection targets, and we used the sub-blocks for subsequent analyses whenever
155 applicable, analyzing a total of 19 selected alleles.
156 Selected haplotype blocks are characterized by a set of marker SNPs which show correlated
157 allele frequency trajectories across replicates. Nevertheless, the correlation is not very stringent
158 to account for sequence diversity among the haplotypes carrying the selection target (Otte and

159 Schlötterer 2019). Hence, not all of the haplotype block marker SNPs describe the frequency
160 trajectory of the (unidentified) selection target equally well. Reasoning that SNPs with the most
161 pronounced allele frequency change are the best representatives of the selection target, we used
162 the 10% most significant marker SNPs of each haplotype block and refer to them as the selected
163 allele. The frequency of each selected allele at every time point is determined as the median
164 frequency of these 10% most significant SNPs. We used only replicates with a selection
165 coefficient large enough to be significantly different from neutrality (p-value < 0.05), therefore
166 we excluded replicates in which a given selected allele did not increase in frequency. The
167 starting frequencies were highly variable among the 19 selected alleles. We detected selected
168 alleles with starting frequency as low as 0.06, but also as high as 0.4 (Figure 2A). The selection
169 coefficients were rather high and ranged from 0.04 to 0.11 (Figure 2A).
170 Overall, we noticed a striking relationship between starting frequency and selection coefficients.
171 Selected alleles starting with lower frequencies had higher selection coefficients than selected
172 alleles with higher starting frequencies. This relationship was significant when analyzing the full
173 set of 19 blocks including the broken-up haplotype blocks (i.e. replacing block 4 and 10 by sub-
174 blocks 4a, 4b, 4c and 10a, 10b, 10c) and was not significantly influenced by block size (linear
175 regression; factor: starting allele frequency p = 0.004 and factor: block size p = 0.130). The
176 inverse relationship between starting allele frequency and selection coefficient was robust with
177 respect to the definition of a selected allele (see Supplementary Figure S1).
178 While a negative correlation between frequency and effect size is expected by theory and has
179 been previously reported for GWAS (Eyre-Walker 2010; Simons et al. 2014; Mancuso et al.
180 2016; Zeng et al. 2018) and E&R (Barghi et al. 2019) studies, it is important to note that a
181 Beavis-like effect (Beavis 1998; Xu 2003) may also contribute to this observation: alleles with
182 low starting frequencies require stronger selection to result in detectable allele frequency
183 changes than alleles starting from intermediate frequencies.

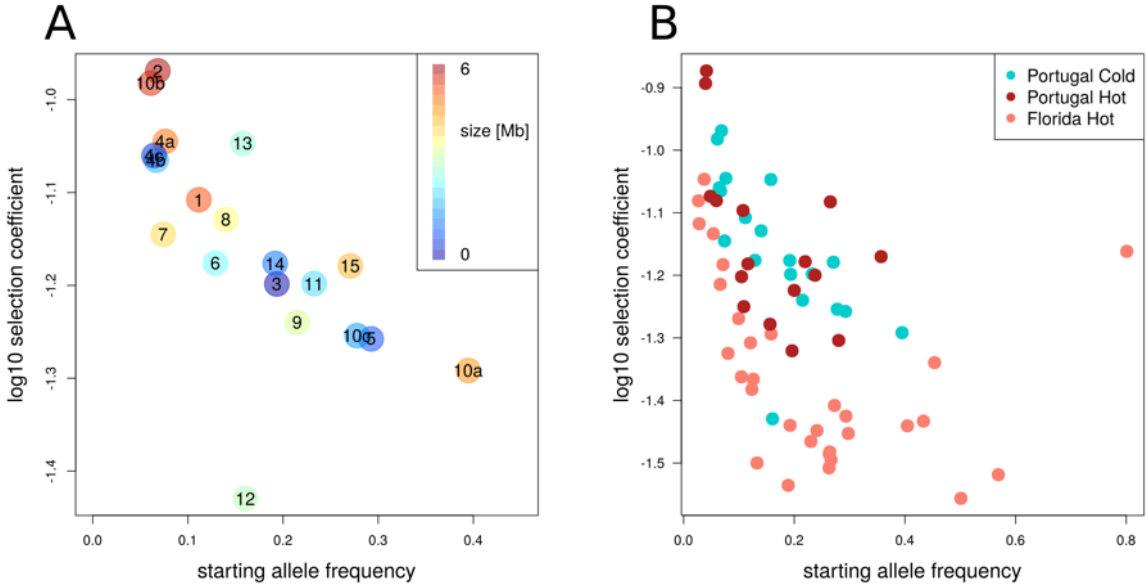


Figure 2: Inverse relationship between starting allele frequency and selection strength. For all experiments, the selected alleles were identified using the same protocol and are based on the top 10% SNPs in reconstructed haplotypes. A) The relationship is shown for the Portugal cold experiment. The color code reflects the size of the selected haplotype block, and starting allele frequencies and selection coefficient of the selection targets are plotted on x- and y-axis. The numbers relate to the selected haplotype blocks from Figure 1B and 1C with numbers indicating blocks detected in the analysis using all time points. Sub-blocks resulting from an analysis using earlier time points are labeled with the letters a, b or c. B) A qualitatively similar relationship between starting allele frequency of each haplotype block and selection strength is found in the cold-evolved Portugal (blue), hot-evolved Portugal (red) and hot-evolved Florida (pink) population. Nevertheless, the distribution in the Florida experiment was shifted towards lower selection coefficients while the two temperature regimes in the Portugal population were highly similar. We conclude that the adaptive architecture is population-specific but does not depend on the temperature regime.

With a median size of 1.5 Mb, the selected haplotype blocks were rather large. The median number of genes per selected haplotype block is 20 but it can reach up to 154 (see Supplementary Figure S2) in the largest reconstructed block (block 2, see Figure 1B). The smallest block contained only a single candidate gene (block number 3, 4.8 kb). All 23 marker SNPs were located within one intronic region of the gene *M-spondin* (*mspo*, FBgn0020269), an extra-cellular matrix protein of *Drosophila*, putatively involved in muscle development (Bataille

203 et al. 2010). The role of this gene in temperature adaption is not apparent and further studies are
204 required for a better understanding of this selection signature.

205 Temperature-specific adaptation

206 Replicates from the same Portuguese founder population were also exposed to a hot selection
207 regime fluctuating between 18°C and 28°C (Mallard et al. 2018). Both temperature regimes have
208 the same daily temperature amplitude of 10°C (cold 10/20°C and hot 18/28°C), but mean
209 temperatures differ (15°C in the cold and 23°C in the hot regime). The temperatures were chosen
210 such that one of the temperatures is stressful, whereas the other temperature is benign (David
211 1983; Petavy et al. 2001). Contrasting the founder population with hot-evolved generation 59,
212 Mallard et al. (2018) identified few (five) very pronounced selection peaks, some of them related
213 to metabolic alterations in the hot-evolved populations.
214 For an unbiased comparison of the two experiments, we added time series data for the hot-
215 evolved populations (F0, F15, F37, F59) and applied the same haplotype reconstruction pipeline
216 as described above. Similar to the cold-evolved population, the X chromosome had too few
217 outlier SNPs (114 SNPs) for haplotype reconstruction. 16 selected haplotype blocks were
218 identified on the two major autosomes (Supplementary Figure S3) and their selection
219 coefficients ranged from 0.05 to 0.13 (Figure 2B). It is remarkable that not only the number of
220 inferred selection targets, but also the distribution of selection coefficients is highly similar for
221 the two temperature regimes (hot-evolved = 16 blocks, cold-evolved = 19 blocks).
222 Only two haplotype blocks shared more SNPs than expected by chance between the two
223 temperature regimes. Furthermore, the shared region was in both cases only a small part of the
224 total haplotype block (Figure 1B and 1C, blocks 2 and 15). A prominent similarity between the
225 selection regimes could be identified in block 15, where the majority of overlapping SNPs were
226 located in the gene *Ace* (FBgn000024). Nevertheless, the selection pattern for *Ace* differs
227 between both temperature regimes (Langmüller et al. 2020). The shared SNPs of block 2 were
228 located in several genes, and therefore no clear candidate for common adaptation could be
229 identified in this region.

230 We further scrutinized the haplotype blocks that were not shared between the selection regimes
231 and had a starting frequency higher than 0.15 to rule out that a selection signature in opposite
232 direction - as expected for a polygenic trait selected in contrasting environments - was missed.
233 The allele frequency change of all candidate SNPs in a haplotype block was always higher in the
234 focal temperature regime. Importantly, in both, hot and cold, selection regimes we very rarely
235 observed a frequency change in the opposite direction (Supplementary Figure S4). We conclude,
236 therefore, that we have no support for alleles being selected in opposite direction in hot and cold
237 temperatures. Rather, most alleles show a temperature-specific response.

238 Population-specific adaptation

239 Independent of the temperature regime the evolved populations derived from the Portugal
240 founder population revealed only a moderate number of selection targets. This contrasts a recent
241 experiment using the same hot temperature regime but a founder population from Florida
242 (Barghi et al. 2019). For a consistent comparison to the Portugal population, we repeated the
243 analysis of the Florida population using our haplotype reconstruction pipeline but focused only
244 on the two major autosomes. 31 selected haplotype blocks were identified on chromosome 2 and
245 3 (Supplementary Figure S5), which are considerably fewer selected alleles than the 88 reported
246 by Barghi et al. (2019) for these two chromosomes. This difference reflects an alternative
247 strategy to identify candidate SNP sets for the haplotype reconstruction rather than the clustering
248 method (Otte and Schlötterer 2019). Following the same protocol as for the Portugal
249 experiments, 9,197 outlier SNPs were identified, which is more conservative than the 52,199
250 outlier SNPs used by Barghi et al. (2019) for haplotype reconstruction. The Florida population
251 harbored about twice as many selected haplotype blocks as the hot-evolved Portugal population.
252 For all experiments we identified the same relationship between starting frequency and selection
253 coefficients, but the distribution for Portugal was shifted towards higher selection coefficients
254 (Figure 2B). This result is robust with respect to the definition of selected alleles (see
255 Supplementary Figure S6). This difference in selection coefficients remains significant when we
256 account for allele frequencies in the founder populations (contrasts between estimated marginal
257 means Portugal cold - Florida hot $p < 0.0001$ and Portugal hot - Florida hot $p < 0.0001$). No

258 significant difference was observed between the two temperature regimes of the Portugal
259 population (Portugal cold - Portugal hot p=0.98).
260 The Florida experiment was based on twice the number of replicates as the Portugal experiment.
261 To rule out that the number of replicates affects the inferred adaptive architecture, we repeated
262 the analysis with 100 sets of five randomly sampled Florida replicates. In all 100 random subsets
263 the selection coefficient was not different from the full data set (Wilcoxon rank-sum test $p > 0.05$
264 adjusted for multiple testing using the Benjamini-Hochberg method), suggesting that the
265 difference between the Portugal and Florida data sets cannot be explained by a different number
266 of replicates.
267 We quantified the degree of parallelism between the experiments using the Jaccard index on the
268 selected haplotype blocks with *s* significantly different from zero. High values indicate parallel
269 genetic responses whereas low values reflect heterogeneous, non-parallel genetic responses
270 between replicates. Jaccard indices were high for the two Portugal experiments (median
271 similarity between replicates 80% and 82%, respectively). For the Florida experiment, the
272 Jaccard index was significantly lower (median similarity between replicates 70% for the full data
273 set; Wilcoxon rank-sum test p-value $< 0.001$ against each Portugal data set), indicating less
274 parallel genetic responses and therefore increased realized genetic redundancy. This pattern was
275 robust with respect to the method used to define a selected allele in a given replicate (Figure 3
276 and Supplementary Figure S7).

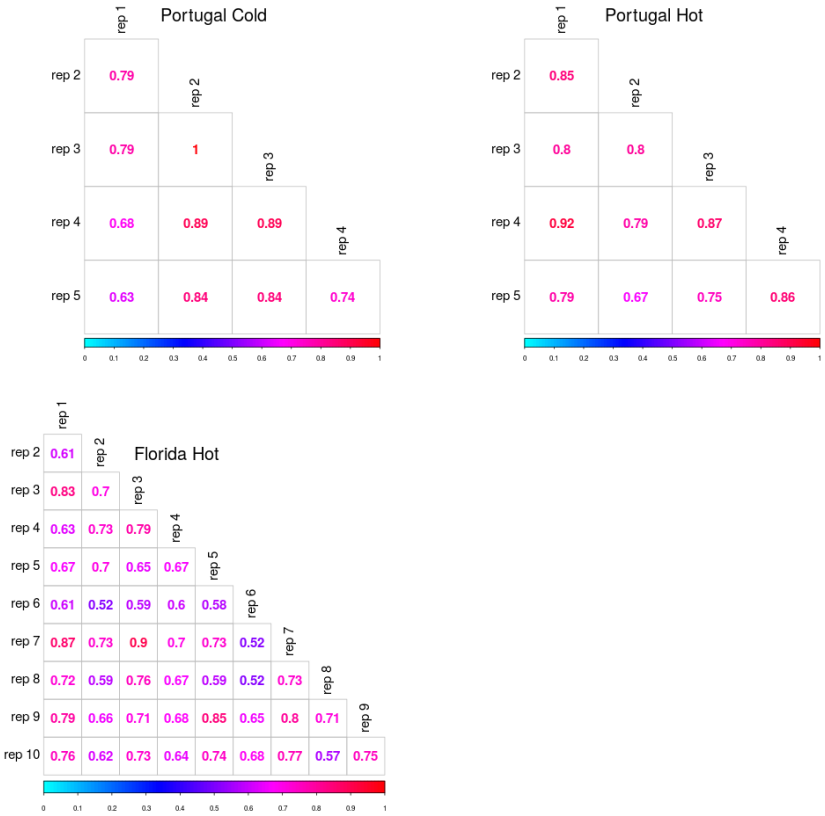


Figure 3: More parallel selection signatures among evolved replicate populations derived from Portugal founders than from those with Florida ancestry. Jaccard indices comparing the different replicates in the cold-evolved Portugal (top left), hot-evolved Portugal (top right) and hot-evolved Florida (bottom) population. Jaccard index was computed based on estimation of significant selection coefficients (p-value $< 0.05$).

The comparison of selected haplotype blocks between evolved populations derived from different founder populations is difficult because the selected haplotype blocks are reconstructed only for significant SNPs. Even if the selected haplotype block is shared, the remaining haplotypes differ between the populations. As the frequency change at a given SNP on the selected haplotype depends on the frequency of this SNP in the non-selected haplotypes, different candidate SNPs are being identified - even if the same haplotype block is selected. Thus, the same selected haplotype block may have different marker SNPs in two different populations - suggesting that different haplotype blocks are selected. Furthermore, the low

290 linkage disequilibrium in natural *Drosophila* populations (Charlesworth and Charlesworth 1973;
291 Langley et al. 1974) implies that very few haplotypes are expected to be shared between samples
292 from different populations. For these reasons, we did not attempt to test whether the same
293 haplotype blocks are selected in Portugal and Florida.

294 **Discussion**

295 *D. simulans* populations of different origin (Portugal and Florida) had very distinct adaptive
296 architectures in the same hot temperature regime (Mallard et al. 2018; Barghi et al. 2019):
297 Portugal had fewer selection targets, which were strongly selected in a highly parallel manner.
298 Florida harbored more selection targets with more heterogeneity among replicates and lower
299 selection coefficients compared to Portugal. In this report, we studied replicate populations
300 derived from the Portugal founder population, which adapted to a cold temperature regime to
301 understand why such different adaptive architectures were inferred in these two populations.
302 Below, we discuss several possible explanations for the differences in adaptive architecture.

303 <u>Different trait optima in the ancestral populations</u>

304 Both founder populations were collected on different locations with their own specific
305 temperature profile and in different phases of the seasonal cycle (Portugal in July 2008, Florida
306 in November 2010). Assuming that temperature adaptation is a single high-level trait, the
307 ancestral trait optimum may differ on the phenotypic axis. This implies that a population, which
308 is less adapted to hot environments should be better adapted to cold environments. Less well
309 adapted populations will experience stronger and more parallel selection responses across
310 replicates (Franssen et al. 2017b; Barghi et al. 2020), consistent with the pattern observed in the
311 hot Portugal population. Different trait optima of the founder populations were further supported
312 by the observation that the Portugal founder population is less fecund than the Florida founder
313 population when assayed in the novel hot environment (Barghi et al., unpublished results). This
314 implies that the mean phenotype of the Portugal population is more distant from the new trait
315 optimum in the hot laboratory environment than the Florida population.

316 The analysis of the cold-evolved replicates casts some doubts on this simple interpretation. We
317 assumed that the hot and cold experiments shifted the trait optimum into opposite directions
318 relative to the (unknown) trait optimum of the ancestral Portugal population. Hence, contributing
319 alleles segregating at sufficiently high frequency in the ancestral population should be selected in
320 opposite direction in the two temperature regimes. Nevertheless, the results did not fit our
321 expectations - most selected haplotype blocks were not shared between the two temperature
322 regimes. While selected haplotype blocks starting from low frequencies may not be identified as
323 selection targets in the opposite temperature regime, also haplotype blocks with higher allele
324 frequencies in the founder population were not selected in opposite direction.
325 Hence, we conclude that temperature adaptation may not be a single high-level phenotype.
326 Rather, several sub-phenotypes on a lower level, which are not all shared for the different
327 temperature regimes, are contributing to adaptation. This conclusion is further supported by
328 different genomic signatures of hot and cold stressors in E&R (Tobler et al. 2014) and QTL
329 mapping (Morgan and Mackay 2006) studies.

330 Differences in adaptive variation

331 Autosomal polymorphism levels differ between the two founder populations with Florida being
332 more variable than Portugal ($\pi_{Florida} = 0.0076$ and $\pi_{Portugal} = 0.0062$, Wilcoxon rank-sum test on
333 non-overlapping 10 kb windows, p-value $< 0.001$). Assuming that neutral variability is a good
334 approximation of adaptive variation, which is not always the case (Kellermann et al. 2009),
335 Portugal is expected to harbor less adaptive variation than Florida. This implies that Florida
336 reaches the trait optimum faster than Portugal (Thornton 2019; Barghi and Schlötterer 2020), but
337 in absence of phenotypic time series data, we cannot assess this hypothesis. A particularly
338 interesting hypothesis related to the different polymorphism levels is that Portugal harbors so
339 little adaptive variation that it does not have much genetic redundancy. This would imply that no
340 (or only limited) excess of adaptive genetic variation is segregating in the Portugal founder
341 population that can be used to reach the trait optimum.

342 The Florida founder population, in contrast, harbors a considerable excess. Such differences in
343 the number of contributing loci can generate quite different patterns of parallel selection
344 responses (Barghi and Schlötterer 2020), matching the Portugal and Florida experiments.
345 Nevertheless, it is not apparent that the moderate differences in genome-wide polymorphism
346 levels are sufficiently large to explain this pattern.

347 Linkage disequilibrium

348 The above discussion about the heterogeneity of the inferred genetic architectures between
349 populations and selection regimes rests on the central assumption that the major contributing loci
350 were identified and could be distinguished with a recently developed haplotype reconstruction
351 approach (Otte and Schlötterer 2019). In other words, it is assumed that only a moderate number
352 of distinct loci contribute to adaptation.
353 Alternatively, the observed selection response may be explained by many loci of small effect -
354 an idea that matches in its extreme form the infinitesimal model (Barton et al., 2017). Empirical
355 support for a highly polygenic architecture of many traits comes from the strong correlation
356 between chromosome length and the fraction of heritability explained (Visscher et al. 2007;
357 Yang et al. 2011; Shi et al. 2016). If multiple small effect loci cluster together this may result in
358 a signature that will be interpreted as a single selection target (Yeaman and Whitlock 2011).
359 Short genomic segments with a local clustering of favored loci can even introgress and leave the
360 strong selection signature of a local allele frequency change (Sachdeva and Barton 2018).
361 Empirical support for the clustering of contributing loci comes from the molecular dissection of
362 candidate loci identified in QTL mapping studies. Single QTL loci can be broken into multiple
363 SNPs contributing to the corresponding trait (Stam and Laurie 1996; King et al. 2012; Kerdaffrec
364 et al. 2016; Gibert et al. 2017; Zan et al. 2017; Shahandeh and Turner 2020).
365 The situation in polymorphic founder populations is significantly more complicated than the
366 simple two genotype case studied by Sachdeva and Barton (2018), but we propose that blocks of
367 linked loci can not only generate pronounced selection signatures, but may also explain the
368 differences in adaptive architecture between the Portugal and Florida experiment. Depending on
369 the extent of linkage disequilibrium (LD) the clustering of contributing loci can vary. Hence,

370 populations with different levels of LD may also harbor more or less clustered contributing loci.
371 The influence of haplotype structure can be illustrated by two extreme cases: in the case of
372 complete linkage equilibrium (LE), in any genomic window the haplotypes segregating in the
373 population should have similar fitness despite being highly diverse. As a consequence, changes
374 in trait optimum will result only in rather small frequency changes of the haplotypes in this
375 genomic window. This pattern becomes more pronounced with an increasing number of
376 contributing loci.
377 On the other hand, in the presence of strong linkage disequilibrium, fewer distinct haplotypes are
378 present in a given genomic window. Sampling variation in the ancestral population generates
379 haplotypes with different numbers of contributing loci in a given genomic window. The more
380 pronounced the difference in the number of loci among haplotypes in a genomic window is, the
381 stronger will be the fitness differences among them and thus the allele frequency change after a
382 shift in trait optimum. Hence, because the difference in the number of contributing loci among
383 haplotypes differs among genomic windows, linkage disequilibrium generates heterogeneity in
384 selection response along the chromosome.
385 We illustrated the impact of LD by assuming about 1200 contributing loci genome-wide and
386 simulated a window size of 1 Mb in a typical E&R setting. For high LD and LE the same
387 number of chromosomes with beneficial alleles was used. 100 different genomic windows were
388 simulated and simulations with higher LD resulted in a more heterogeneous response to
389 selection. Consistent with a larger phenotypic variance (Figure 4A) also much more pronounced
390 allele frequency changes were observed for some windows in the presence of linkage
391 disequilibrium (Figure 4B). Hence, while very homogeneous moderate frequency shifts were
392 observed for beneficial alleles in linkage equilibrium, some pronounced sweep windows were
393 detected for windows with LD. We also assessed the degree of parallelism in the response
394 between replicates and found a more parallel response for the high LD simulations (Figure 4C).

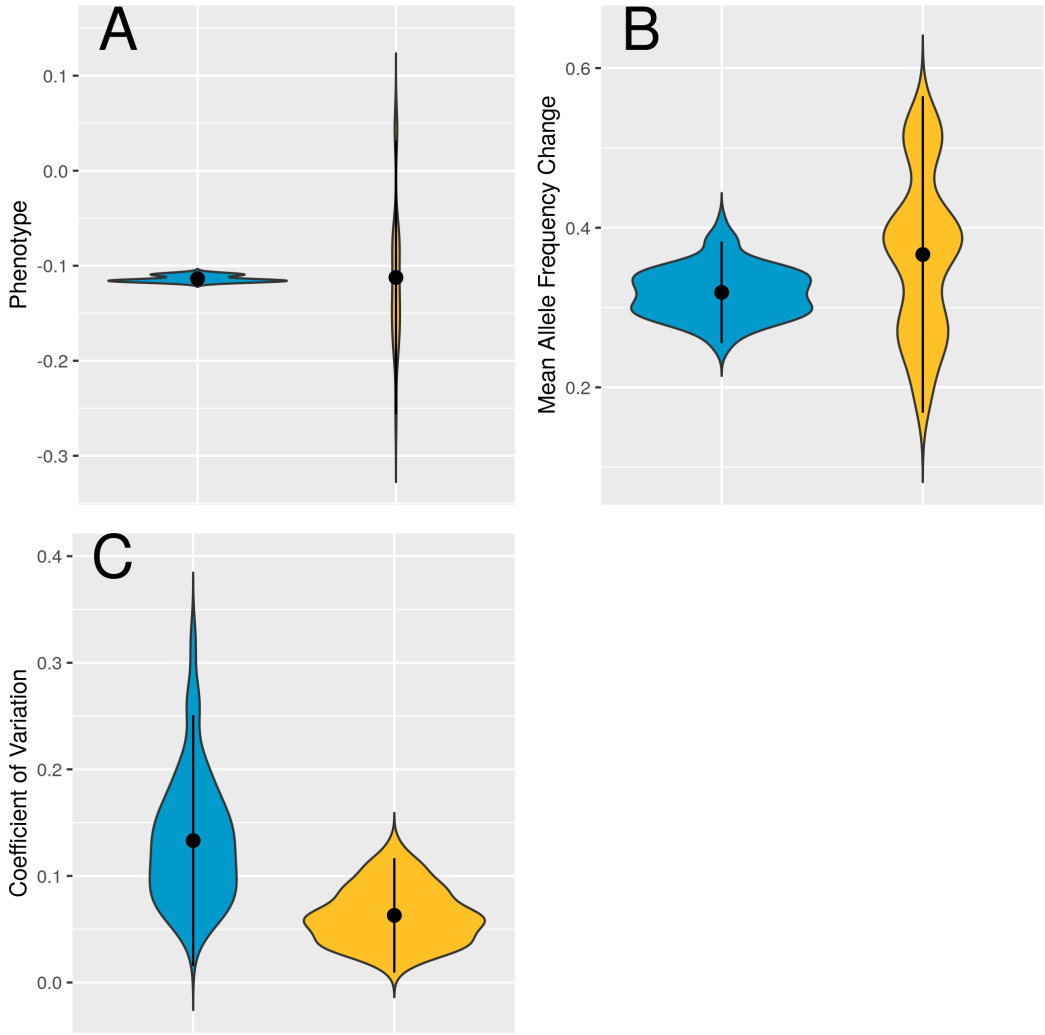


Figure 4: Influence of linkage disequilibrium on the genomic response of a polygenic trait. We simulated 50 generations of polygenic adaptation after a shift in trait optimum. 100 replicates, each with 10 loci in a 1 Mb region either with linkage equilibrium (blue) or strong LD (yellow) are shown in violin plots. A) Independent of linkage structure, the same mean phenotype was reached, but simulations with high LD were considerably more scattered. B) Pronounced allele frequency changes were obtained for both, linkage equilibrium und high LD. For linkage equilibrium, the genomic windows were all rather similar, indicating that no window showed a strong selection signature distinguishing it from the genomic background. Simulations with strong LD, however, resulted in highly heterogeneous selection responses, with some windows having a frequency change larger than 0.6, which is a strong selection signature distinguishing it from the remaining genomic windows. C) The heterogeneity among five replicate populations is measured by the coefficient of variation. The selection response in simulations with linkage equilibrium was less parallel than in those with strong LD.

407 Thus, for polygenic traits the inferred adaptive architecture can be strongly affected by linkage in
408 the ancestral population. A previous study on the impact of recombination on the response to a
409 shift in trait optimum with truncating selection observed more heterogeneity among replicates in
410 the case of linkage equilibrium than for complete linkage (Zhang and Hill 2005). We attribute
411 these differences to the small population sizes in Zhang and Hill (2005).
412 Nevertheless, does this scenario of a highly polygenic architecture with differences in LD apply
413 to the Florida and Portugal experiments? Following the same rationale as Shi et al. (2016),
414 Barghi et al. (2019) tested whether longer haplotype blocks were more strongly selected than
415 shorter ones, but no significant correlation was found. Similar results were observed for the cold
416 evolved Portugal populations. We caution, however, that these negative results do not provide
417 strong support for the identification of distinct selection targets. Possible, not mutually exclusive,
418 reasons for the lack of significance even in the presence of a highly polygenic architecture are:
419 1) the contributing loci have different effect sizes, thus small haplotype blocks with large effect
420 loci may be more strongly selected ones than larger blocks, 2) larger blocks may harbor more
421 loci with effects in opposite direction than smaller ones, 3) since haplotype blocks are still
422 relatively short (compared to full chromosomes) stochastic sampling and heterogeneity in the
423 density of contributing loci may obscure the correlation between size of the selected haplotype
424 block and the selection response.
425 The hypothesis that LD differences can explain the heterogeneity in inferred adaptive
426 architecture is supported by the observation that the two founder populations differed across all
427 chromosomes in their pattern of linkage disequilibrium (Figure 5). The higher LD in Portugal
428 compared to Florida is fully consistent with the prediction that founder populations with higher
429 LD are more likely to show stronger and more parallel sweep signatures than populations with
430 lower LD. Although this pattern fits our observations, in absence of more information about the
431 degree of polygenicity and the distribution of contributing loci across the chromosomes and their
432 effect sizes, it is not possible to determine whether the observed differences in LD are sufficient
433 to explain our empirical data.

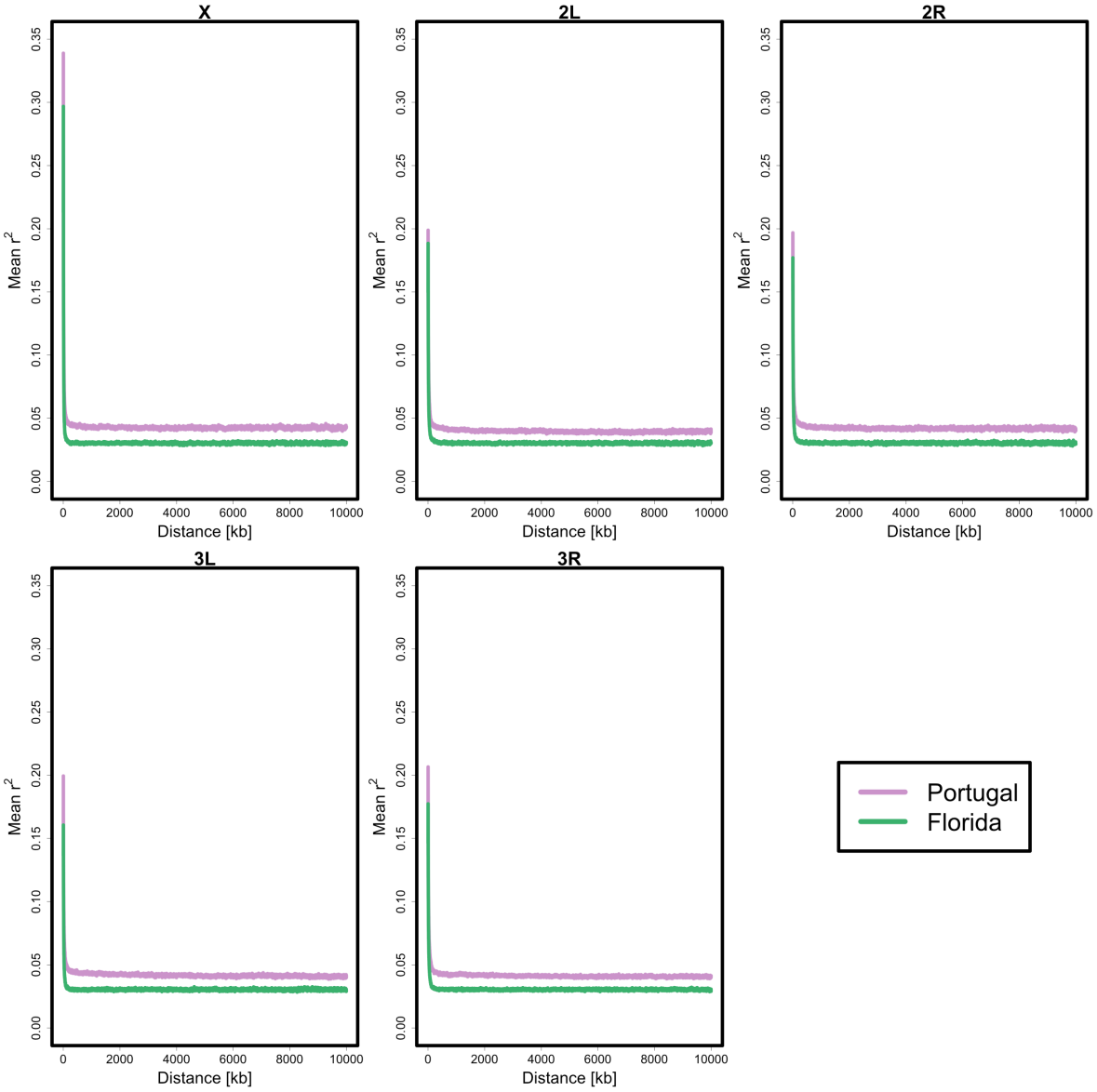


434 Figure 5: Linkage disequilibrium in the ancestral Portugal und Florida population as measured by the
435 mean $r^2$ of loci with distances up to 10,000 kb based on 34 individual haplotype sequences.

436 Temperature adaptation may involve multiple, temperature-specific traits
437 While we cannot pinpoint the cause for the differences in the inferred adaptive architecture
438 between Portugal and Florida, the analysis of cold-evolved replicates shed some important light
439 on our understanding of temperature adaptation.
440 Many studies, in particular theoretical ones, considered high level phenotypes, such as
441 temperature adaptation, as a single adaptive trait, where shifts in mean temperature are treated as
442 a simple shift in trait optimum (e. g. Bridle et al. 2009; Chevin et al. 2010; Hoffmann 2010;
443 Kopp and Matuszewski 2014). This implies that all segregating contributing loci affect the
444 optimal phenotype - irrespective of the position of the optimum - i.e. in the case of temperature
445 adaptation irrespective of whether the optimum is in the hot or cold. The limited overlap between
446 the selection targets in hot- and cold-evolved replicates is striking, as it contradicts this
447 assumption. With the exception of the genomic region around the *Ace* locus and a region across
448 the centromere of chromosome 2, which changed in the same direction in both temperature
449 regimes, no shared haplotype blocks were detected. To some extent, the lack of shared haplotype
450 blocks can be attributed to low starting frequencies, which implies that selection in the opposite
451 direction does not result in allele frequency changes sufficiently large to be detected.
452 Nevertheless, even for haplotype blocks starting from intermediate frequency, no selection
453 signature in the opposite direction was noticed.
454 This implies that different loci are contributing to adaptation in hot and cold environments -
455 irrespective of whether a highly or moderately polygenic architecture is assumed. A very similar
456 lack of shared candidates was also noticed in a *D. melanogaster* experiment, where replicate
457 populations were exposed to the same hot and cold temperature regimes (Tobler et al. 2014).
458 This experiment was, however, conducted for a much smaller number of generations, and the
459 selection signature was analyzed on the SNP-level, which makes the interpretation of the results
460 particularly challenging given the contribution of large segregating inversions to temperature
461 adaptation in this species (Hoffmann et al. 2002; Rako et al. 2007).
462 The observation of different selection targets in hot and cold environments is particularly
463 interesting, because seasonal changes were found to be associated with cycling allele frequencies
464 in natural *D. melanogaster* populations (Bergland et al. 2014), which suggests that the same

465 SNPs are being selected in opposite direction in hot and cold environments. One possible
466 explanation for these differences to our study is that in natural populations only a moderate
467 number of generations separates the two temperature regimes, while in our experiment the
468 temperature regime remained constant across more than 50 generations.

469 Population-specific adaptive architectures

470 Various studies, mainly using QTL mapping and GWAS, have identified different loci
471 contributing to the same trait in diverged populations (Adeyemo et al. 2009; Wu et al. 2013; Al
472 Olama et al. 2014; Li and Keating 2014; Conte et al. 2015; Horikoshi et al. 2018; Takata et al.
473 2019; Wojcik et al. 2019; Zan and Carlborg 2019; Hodonsky et al. 2020; Kemppainen et al.
474 2020). A recent experimental evolution study using *D. subobscura* populations with different
475 genetic background also observed very little overlap in the genomic regions responding to a
476 common selection regime (Seabra et al. 2018). Hence, the different selection targets obtained
477 from Portugal and Florida experiments conducted in the same hot environment are not
478 particularly surprising and emphasize the limited insights about the genetic basis of a polygenic
479 trait from single population studies. Very surprising, however, was the observation that the
480 adaptive architecture (number of contributing loci, effect sizes and starting frequencies) was
481 different between Portugal and Florida, but strikingly similar between the hot and cold selection
482 regime.

483 Although more experiments are needed to nail down why the adaptive architecture is highly
484 dependent on the founder population and not on the selection regime, our results have important
485 implications for all studies attempting to characterize the adaptive architecture. The analysis of a
486 single population cannot be sufficient to understand the genetic basis of adaptive traits. Thus,
487 multiple diverged populations need to be studied to reach conclusions that can be generalized
488 beyond a limited number of focal populations.

489 **Material and Methods**

490 Unless stated otherwise, analysis was conducted using R v3.6.1 (R Core Team 2019).

491 Experimental Populations and Selection Regime

492 The set-up of the evolution experiment is described in detail elsewhere (Mallard et al. 2018). In
493 brief, female flies were sampled from a natural *Drosophila simulans* population in Northern
494 Portugal in the summer of 2008 and used to establish 250 isofemale lines. These lines were kept
495 for 10 generations in the laboratory before starting the experiment. Mated females of all lines
496 were used to create the starting populations. Ten replicates were created by combining an equal
497 number of flies from each line. Five of the replicates were then kept in a 12h:12h day and night
498 cycle with temperatures of 20°C during the day and 10°C during the night (*cold regime*). The
499 population size was kept constant at 1250 per replicate in non-overlapping generations.
500 The other five replicates were used to start the evolution experiment described by Mallard et al.
501 (2018), which was identical to the cold regime except for the temperature which fluctuated
502 between 28°C during the day and 18°C at night (*hot regime*).

503 Evolve & Resequence

504 For the founder population, we used the sequences described by Mallard et al. (2018), but added
505 new sequence data from two replicates of generation F3 from the cold regime to increase
506 coverage. To avoid biases related to different sequencing approaches, all reads were pooled and
507 then randomly split into five subsets with a coverage of 100x each. These subsets were used as
508 founder population replicates throughout the analysis of the cold-evolved and the (re-)analysis of
509 the hot-evolved populations. While sequence data for the F59 in the hot regime were available
510 from Mallard et al. (2018), we added new Pool-Seq data for the intermediate time points F15 and
511 F37 in the hot regime to allow for the time series analysis and haplotype reconstruction in this
512 study. All sequences used for the founder population (including the F3 from the cold regime) and
513 all sequences of the hot regime were derived from females only.

514 Sequencing data from the time points F11, F21, F31, F41 and F51 in the cold regime were newly
515 generated from pooled females and males. Paired-end libraries were generated with different
516 protocols and sequenced on different Illumina platforms (see Supplementary Table S1).

517 Data processing

518 Sequencing reads were trimmed using Readtools TrimFastq version 0.2. (Gomez-Sanchez and
519 Schlötterer 2017) with the parameters --minReadLength 50 --disable5pTrim --
520 mottQualityThreshold 20. The *D. simulans* genome sequence created by Palmieri et al. (2015)
521 was used as reference for read mapping. To avoid false positive outlier SNPs, which might arise
522 when libraries with different read lengths and insert sizes are combined in one analysis (Kofler et
523 al. 2016), three different mappers were used to map reads of the two time points used for outlier
524 testing (cold regime: F0 and F51; hot regime: F0 and F59). Reads were mapped using Bowtie2
525 version 2.2.6 (Langmead and Salzberg 2012) with parameters --end-to-end --X 1500, bwa mem
526 version 0.7.13 (Li and Durbin 2010) with default parameters and novoalign version 3.03.2
527 (Novocraft 2014) with parameters -i 350,100 -F STDFQ -o SAM -r RANDOM.
528 The intermediate time points (cold regime: F11, F21, F31, F41; hot regime F15, F37) used for
529 the detection of selected haplotype blocks were mapped with novoalign only, as this mapper is
530 known to estimate allele frequencies most accurately (Kofler et al. 2016).
531 Mapped reads were filtered for mapping quality ≥ 20 and proper pairs using SAMtools view
532 version 1.3.1 (Li et al. 2009). Duplicates were removed using picard MarkDuplicates version
533 2.1.1 (Broad Institute 2019). Barcoded files were split using Readtools
534 AssignReadGroupByBarcode version 0.2.2 (Gomez-Sanchez and Schlötterer 2017) with
535 parameters --maximumMismatches 1. The BAM files were then used to create mpileup files with
536 SAMtools mpileup version 1.3.1 (Li et al. 2009), and finally, PoPoolation2 mpileup2sync.jar
537 version 1.201 (Kofler et al. 2011) was used to create sync files from mpileup files. All
538 subsequent analysis was conducted on the basis of these sync files.

539 SNP calling and masking

540 Single nucleotide polymorphisms (SNPs) were called from the founder population by creating
541 sync files from BAM files as described above but filtering for polymorphic sites that had a
542 mapping quality of at least 30 and a minimal count of at least 5 and were detected by the three
543 mapping algorithms in all founder replicates. Filtering resulted in 3.8 million SNPs that were
544 used for further analysis. Indels were detected using the PoPoolation2 identify-indel-regions.pl
545 script, and transposable elements were detected with repeatmasker v 1.332 (Smit et al. 2015).
546 Custom databases made by combining RepeatMasker database Dfam_Consensus-20181026,
547 RepBase-20181026, and transposon_sequence_set.embl.txt from flybase.org (FB 2018_06), and
548 search engine NCBI/RMBLAST v 2.2.27+ were used for repeats > 500 bp. All sync files were
549 masked for these repetitive regions and for known Y chromosome translocations (Tobler et al.
550 2017) using the PoPoolation2 filter-sync-by-gtf.pl script.

551 Correcting for different insert sizes

552 To correct for false positive outlier SNPs created by libraries with different insert sizes (Kofler et
553 al. 2016), mapping results from the three different mappers for the founder (F0) and most
554 evolved (cold regime: F51; hot regime F59) population were used. $\chi^2$ tests were conducted to
555 compare the results of the different mappers per replicate and time point. After correcting for
556 multiple testing using the Benjamini-Hochberg procedure (Benjamini and Hochberg 1995), only
557 SNPs that showed a consistent response across comparisons (p.adjust $\geq$ 0.05) were kept for
558 further analysis.

559 Candidate SNPs

560 Candidate outlier SNPs were detected in the filtered sync files created from novoalign mapping
561 results after correcting for false positive outliers as described above. Allele frequency changes
562 between the founder and the most evolved population were analyzed using CMH and $\chi^2$ tests
563 which are adapted for genetic drift and pool sequencing noise as implemented in the R package
564 ACER version 1.0 (Spitzer et al. 2020). SNPs within the top 1% of coverage were excluded from

565 the analysis to avoid copy number variants. Intermediate generations were included in the
566 correction approach. Effective population size per replicate was calculated using the R package
567 poolSeq version 0.3.5 (Taus et al. 2017) with the function estimateWndNe (window size *10 kb*,
568 method *P.planI*, pool size and census size *1250*) and used for CMH and $\chi^2$ tests. The CMH test
569 was performed using all population replicates per time point whereas $\chi^2$ tests were performed for
570 each replicate separately. All results were corrected for multiple testing (Benjamini-Hochberg).
571 Finally, candidate SNPs detected by either test (p.adjust < 0.05) were combined to include
572 consistent responses across replicates (CMH test) and replicate-specific responses ($\chi^2$ test).

573 Selected haplotype blocks

574 Selected haplotype blocks were reconstructed from candidate SNP allele frequency data of all
575 time points and replicates using the R package haplovalidate with MNCS of 0.01 (Otte and
576 Schlötterer 2019). Haplotype blocks were reconstructed for all time points. As haplotype blocks
577 might contain more than one selected allele, early time points (cold regime: F11, F21 and F31;
578 hot regime: F15 and F37) were used for fine-mapping of selected haplotype blocks (Otte and
579 Schlötterer 2019). Here, the analysis detected the characteristic signal of reconstructed haplotype
580 blocks with multiple selection targets, which is the presence of a single haplotype block in the
581 most evolved generation but several reconstructed haplotype blocks when analyzing the early
582 generations separately. Haplotype blocks from the early generations showing this pattern were
583 included in the final analysis.
584 Selection coefficients for the detected haplotype blocks per replicate were computed using the
585 allele frequency trajectories of the top 10% outlier SNPs based on CMH and $\chi^2$ test result and
586 using the poolSeq v0.3.5 function estimateSH (method *LLS*) (Taus et al. 2017). Only selection
587 coefficients with p-value < 0.05 were used to calculate the median selection coefficient for each
588 selected allele. Relationship of selection coefficient, starting allele frequency and block size were
589 tested using a linear model with log10 transformation of selection coefficients. To test the
590 robustness of our definition for selected alleles, we repeated the estimation of selection
591 coefficients using a) the top 20% SNPs or b) all SNPs that had an allele frequency change > 0.1
592 (Supplementary Figure S1). Candidate genes per block were detected from the gene annotation

593 of the reference genome (Palmieri et al. 2015) including also SNPs 200 bp up- and downstream
594 of the focal gene.

595 Comparison to other experimentally evolved *D. simulans* populations

596 We used data from the same *D. simulans* population evolving under a hot temperature regime
597 (Mallard et al. 2018) to contrast adaptation to different temperatures. For this population, we
598 included two additional time points, so that four time points in total were available: F0, F15,
599 F37, F59. The data set was filtered, candidate SNPs were detected and haplotypes were
600 reconstructed in the same way as described above including the combined analysis of all (F0-
601 F59) and early (F0-F37) time points. To estimate how many shared marker SNPs were expected
602 by chance, we randomly sampled the number of shared SNPs from the haplotype blocks,
603 calculated the fraction per haplotype block (N=10,000) and finally applied a 95 % cut-off.
604 In addition, a different published hot-evolved *D. simulans* population from Florida (Barghi et al.
605 2019) was used for the comparative analysis. The data set was filtered and candidate SNPs were
606 detected in the same way as described above. As intermediate time points were available for this
607 data set (every 10th generation from F0 to F60), haplovalidate (Otte and Schlötterer, 2019) with
608 MNCS of 0.01 was used to detect selected haplotype blocks including the combined analysis of
609 all (F0-F60) and early (F0-F30) time points as described for the Portugal population. Selection
610 coefficients were computed as described above.
611 We fitted a linear model with log10 transformed selection coefficients as response and main
612 effects of population as fixed categorical effect with three levels (Florida hot, Portugal hot,
613 Portugal cold) and a linear and quadratic covariate for starting allele frequency, to account for
614 their non-linear relationship with the response, as explanatory variables. Residuals from this
615 model were normally distributed and displayed variance homogeneity. The model with linear
616 and quadratic covariate for starting allele frequency fit significantly better than a model with
617 only a linear term. Contrasts between populations were compared based on estimated marginal
618 means (R package *emmeans*).
619 We compared the similarity of replicates calculating the Jaccard indices for the Portugal and the
620 Florida population using the R package *philentropy* (Drost 2018). We created binary data based

621 on the replicate-specific selection response, i.e. whether or not a significant selection coefficient
622 could be estimated by the poolSeq package (see above) for the corresponding replicate and allele
623 (p-value <0.05). Following Barghi et al. (2019), we created binary data by applying a cut-off of
624 0.1 to the median allele frequency change of selected alleles per replicate. Jaccard indices
625 between populations were compared using the two-sample Wilcoxon rank-sum test. To analyze
626 the effect of the different number of replicates (10 in the Florida and five in the Portugal
627 population) we repeated the analysis of selection coefficients and Jaccard indices on a
628 downsampled set of Florida replicates. For this analysis, we took 100 random samples of five
629 replicates from the Florida population data set and repeated the analysis for each of them as
630 described above.

631 Nucleotide diversity in the ancestral populations

632 Nucleotide diversity ($\pi$) of each autosome in the ancestral populations was calculated from the
633 allele frequency data using the formula of Tajima (1989). For maintaining a comparable number
634 of low-frequency alleles we subsampled the Florida data set to five replicates. As different sets
635 of five Florida replicates resulted in very consistent $\pi$ estimates (data not shown) we only used
636 one set for the direct comparison to Portugal.

637 Linkage disequilibrium in the ancestral populations

638 To quantify linkage disequilibrium, we used 189 haplotype sequences of the Florida founder
639 population (Howie et al. 2019) and 34 haplotype sequences of the Portugal founder population
640 which are described in Langmüller et al. (2020). For maintaining a comparable number of low-
641 frequency alleles, we subsampled the Florida data set to 34 haplotypes. We calculated the mean
642 $r^2$ for loci (minor allele count = 3, minimum SNP quality = 50) within 10,000 kb distance. As
643 different sets of 34 Florida haplotypes resulted in very consistent mean estimates (see
644 Supplementary Figure S8) we only used one set for the direct comparison to Portugal.

645 Linkage disequilibrium simulations

646 We illustrated the effect of linkage equilibrium (LE) or strong linkage disequilibrium (LD) on
647 polygenic adaptation after a shift in trait optimum with computer simulations using MimicrEE2
648 v208 (Vlachos and Kofler 2018) in qff mode. We used parameters that matched the Portugal *D.*
649 *simulans* E&R experiment with five replicates, each starting with the same 1000 homozygous
650 individuals which evolved for 50 generations. For computational simplicity, we assumed that all
651 10 loci contributing to the phenotype, each with a starting allele frequency of 0.05 and effect size
652 of 0.05, are restricted to a 1 Mb region. 100 independent simulations were performed to mimic
653 100 different genomic regions. We used a Gaussian fitness function as previously described (e.g.
654 Barghi and Schlötterer 2020): minimum fitness 0.5, maximum fitness 4.5, standard deviation of
655 the phenotype 1.2, heritability of 0.5. The mean fitness of the ancestral population was -0.44 and
656 the new trait optimum was 0.5. We used the average recombination rate of *D. simulans*
657 (Dsim_recombination_map_LOESS_100kb_1.txt, (Howie et al. 2019)). We generated two
658 different sets of founder populations, one with strong LD and one with linkage equilibrium (LE).
659 Both sets of founder populations contained 200 chromosomes with favored alleles and 800
660 chromosomes without. For strong LD, four different sets of selected haplotypes were generated,
661 and the number of contributing loci was randomly distributed between the four sets of selected
662 haplotypes. Hence, 50 haplotypes had the same number of contributing loci, but due to stochastic
663 sampling the number of contributing loci differs among the four sets of 50 haplotypes. To
664 generate starting populations in LE, we randomly distributed the selected alleles across 200
665 haplotypes until each of the alleles had a final frequency of 0.05.
666 After 50 generations, we generated "Pool-seq data" with 50x coverage and added sequencing
667 noise by binomial sampling based on the allele frequencies. We recorded the phenotypic and
668 mean frequency change across loci and replicates as well as the coefficient of variation in the
669 mean allele frequency change across the five replicates as an indicator for the degree of parallel
670 response.

671 **Data Availability**

672 Sequence data were deposited at the European Nucleotide Archive (ENA) under the accession
673 number XXX. Population sync files, all results and scripts were deposited on Dryad Digital
674 Repository XXX.

675 **Acknowledgments**

676 We thank Neda Barghi for sharing unpublished fecundity data and for providing information
677 concerning the hot-evolved *D. simulans* data set. Anna Langmüller, Thomas Taus and Claire
678 Burny shared code to remove SNPs with allele frequency estimates that are sensitive to the insert
679 sizes of NGS sequencing libraries. The authors also thank the members of the Institute of
680 Population Genetics for discussion and support on the project. Special thanks to Marlies Dolezal
681 for in depth statistical advice. KAO was supported by a DFG Research Fellowship (OT 532/1-1).
682 FM was supported by a Marie Sklodowska-Curie Individual Fellowship (H2020-MSCA-IF-
683 661149). CS was supported by the European Research Council grant "ArchAdapt" and the
684 Austrian Science Funds (FWF, P27630, P29133). Illumina sequencing for a subset of the data
685 was performed at the VBCF NGS Unit (www.viennabiocenter.org/facilities).

686 **References**


687 Adeyemo A, Gerry N, Chen G, Herbert A, Doumatey A, Huang H, Zhou J, Lashley K, Chen Y,
688 Christman M et al. 2009. A genome-wide association study of hypertension and blood
689 pressure in African Americans. *PLoS Genet* **5**: e1000564.
690 Al Olama AA Kote-Jarai Z Berndt SI Conti DV Schumacher F Han Y Benlloch S Hazelett DJ
691 Wang Z Saunders E et al. 2014. A meta-analysis of 87,040 individuals identifies 23 new
692 susceptibility loci for prostate cancer. *Nat Genet* **46**: 1103-1109.
693 Barghi N, Hermisson J, Schlötterer C. 2020. Polygenic adaptation: a unifying framework to
694 understand positive selection. *Nature reviews Genetics*: in press.
695 Barghi N, Schlötterer C. 2020. Distinct patterns of selective sweep and polygenic adaptation in
696 evolve and re-sequence studies. *Genome biology and evolution* doi:10.1093/gbe/evaa073.
697 Barghi N, Tobler R, Nolte V, Jaksic AM, Mallard F, Otte KA, Dolezal M, Taus T, Kofler R,
698 Schlötterer C. 2019. Genetic redundancy fuels polygenic adaptation in *Drosophila*. *PLoS*
699 *biology* **17**: e3000128.
700 Barton NH, Etheridge AM, Veber A. 2017. The infinitesimal model: Definition, derivation, and
701 implications. *Theoretical population biology* **118**: 50-73.
702 Barton NH, Keightley PD. 2002. Understanding quantitative genetic variation. *Nature reviews*
703 *Genetics* **3**: 11-21.
704 Bataille L, Delon I, Da Ponte JP, Brown NH, Jagla K. 2010. Downstream of identity genes:
705 muscle-type-specific regulation of the fusion process. *Dev Cell* **19**: 317-328.
706 Beavis WD. 1998. *QTL analyses: power, precision, and accuracy*.
707 Benjamini Y, Hochberg Y. 1995. Controlling the false discovery rate: a practical and powerful
708 approach to multiple testing. . *J R Stat Soc Ser* **57**: 289–300.
709 Bergland AO, Behrman EL, O'Brien KR, Schmidt PS, Petrov DA. 2014. Genomic evidence of
710 rapid and stable adaptive oscillations over seasonal time scales in *Drosophila*. *PLoS*
711 *genetics* **10**: e1004775.
712 Bridle JR, Gavaz S, Kennington WJ. 2009. Testing limits to adaptation along altitudinal
713 gradients in rainforest Drosophila. *Proceedings Biological sciences / The Royal Society*
714 **276**: 1507-1515.
715 Broad Institute. 2019. Picard toolkit. http://broadinstitute.github.io/picard/.
716 Bulmer MG. 1971. Effect of Selection on Genetic Variability. *Am Nat* **105**: 201-&.
717 Charlesworth B, Charlesworth D. 1973. A study of linkage disequilibrium in populations of
718 Drosophila melanogaster. *Genetics* **73**: 351-359.
719 Chevin LM, Lande R, Mace GM. 2010. Adaptation, plasticity, and extinction in a changing
720 environment: towards a predictive theory. *PLoS biology* **8**: e1000357.
721 Conte GL, Arnegard ME, Best J, Chan YF, Jones FC, Kingsley DM, Schluter D, Peichel CL.
722 2015. Extent of QTL Reuse During Repeated Phenotypic Divergence of Sympatric
723 Threespine Stickleback. *Genetics* **201**: 1189-1200.
724 David JR, Allemand, R., Van Herrewege, J. and Cohet, Y. . 1983. Ecophysiology: abiotic
725 factors. In *The Genetics and Biology of Drosophila*, Vol 3d (ed. M Ashburner, Carson, H.
726 L. & Thompson, J. N. Jr ), pp. 105–170. Academic Press, London.

727 de Vladar HP, Barton N. 2014. Stability and response of polygenic traits to stabilizing selection
728 and mutation. *Genetics* **197**: 749-767.
729 Drost HG. 2018. Philentropy: Information Theory and Distance Quantification with R. *Journal*
730 *of Open Source Software* **3**: 765.
731 Eyre-Walker A. 2010. Evolution in health and medicine Sackler colloquium: Genetic
732 architecture of a complex trait and its implications for fitness and genome-wide
733 association studies. *Proc Natl Acad Sci U S A* **107 Suppl 1**: 1752-1756.
734 Field Y, Boyle EA, Telis N, Gao Z, Gaulton KJ, Golan D, Yengo L, Rocheleau G, Froguel P,
735 McCarthy MI et al. 2016. Detection of human adaptation during the past 2000 years.
736 *Science* **354**: 760-764.
737 Fisher RA. 1918. The correlation between relatives on the supposition of Mendelian Inheritance.
738 *Trans Roy Soc Edinburgh* **52**: 339-433.
739 Flint J, Mott R. 2001. Finding the molecular basis of quantitative traits: successes and pitfalls.
740 *Nat Rev Genet* **2**: 437-445.
741 Franssen SU, Barton NH, Schlötterer C. 2017a. Reconstruction of haplotype-blocks selected
742 during experimental evolution. *Molecular biology and evolution* **118**: 42-51.
743 Franssen SU, Kofler R, Schlötterer C. 2017b. Uncovering the genetic signature of quantitative
744 trait evolution with replicated time series data. *Heredity* **118**: 42-51.
745 Garland T, Rose MR. 2009. *Experimental Evolution: concepts, methods, and applications of*
746 *selection experiments*. University of California Press, Berkeley.
747 Gazal S, Finucane HK, Furlotte NA, Loh PR, Palamara PF, Liu X, Schoech A, Bulik-Sullivan B,
748 Neale BM, Gusev A et al. 2017. Linkage disequilibrium-dependent architecture of human
749 complex traits shows action of negative selection. *Nature genetics* **49**: 1421-1427.
750 Gibert JM, Blanco J, Dolezal M, Nolte V, Peronnet F, Schlötterer C. 2017. Strong epistatic and
751 additive effects of linked candidate SNPs for Drosophila pigmentation have implications
752 for analysis of genome-wide association studies results. *Genome biology* **18**: 126.
753 Gomez-Sanchez D, Schlötterer C. 2017. ReadTools: A universal toolkit for handling sequence
754 data from different sequencing platforms. *Molecular ecology resources*
755 doi:10.1111/1755-0998.12741.
756 Harris AM, DeGiorgio M. 2020. Identifying and Classifying Shared Selective Sweeps from
757 Multilocus Data. *Genetics* **215**: 143-171.
758 Hodonsky CJ, Baldassari AR, Bien SA, Raffield LM, Highland HM, Sitlani CM, Wojcik GL,
759 Tao R, Graff M, Tang W et al. 2020. Ancestry-specific associations identified in genome-
760 wide combined-phenotype study of red blood cell traits emphasize benefits of diversity in
761 genomics. *BMC Genomics* **21**: 228.
762 Hoffmann AA. 2010. Physiological climatic limits in *Drosophila*: patterns and implications. *J*
763 *Exp Biol* **213**: 870-880.
764 Hoffmann AA, Anderson A, Hallas R. 2002. Opposing clines for high and low temperature
765 resistance in *Drosophila melanogaster*. *Ecol Lett* **5**: 614-618.
766 Höllinger I, Pennings PS, Hermisson J. 2019. Polygenic adaptation: From sweeps to subtle
767 frequency shifts. *PLoS genetics* **15**: e1008035.

768 Horikoshi M, Day FR, Akiyama M, Hirata M, Kamatani Y, Matsuda K, Ishigaki K, Kanai M,
769 Wright H, Toro CA et al. 2018. Elucidating the genetic architecture of reproductive
770 ageing in the Japanese population. *Nat Commun* **9**: 1977.
771 Howie JM, Mazzucco R, Taus T, Nolte V, Schlotterer C. 2019. DNA motifs are not general
772 predictors of recombination in two Drosophila sister species. *Genome biology and*
773 *evolution* doi:10.1093/gbe/evz082.
774 Jain K, Stephan W. 2017a. Modes of rapid polygenic adaptation. *Molecular biology and*
775 *evolution* **34**: 3169-3175.
776 Jain K, Stephan W. 2017b. Rapid Adaptation of a Polygenic Trait After a Sudden Environmental
777 Shift. *Genetics* **206**: 389-406.
778 Jensen JD, Kim Y, DuMont VB, Aquadro CF, Bustamante CD. 2005. Distinguishing between
779 selective sweeps and demography using DNA polymorphism data. *Genetics* **170**: 1401-
780 1410.
781 Jha AR, Miles CM, Lippert NR, Brown CD, White KP, Kreitman M. 2015. Whole-genome
782 resequencing of experimental populations reveals polygenic basis of egg-size variation in
783 *Drosophila melanogaster*. *Molecular biology and evolution* **32**: 2616-2632.
784 Jha AR, Zhou D, Brown CD, Kreitman M, Haddad GG, White KP. 2016. Shared Genetic Signals
785 of Hypoxia Adaptation in Drosophila and in High-Altitude Human Populations. *Mol Biol*
786 *Evol* **33**: 501-517.
787 Johnson KE, Voight BF. 2018. Patterns of shared signatures of recent positive selection across
788 human populations. *Nat Ecol Evol* **2**: 713-720.
789 Johri P, Charlesworth B, Jensen JD. 2020. Toward an Evolutionarily Appropriate Null Model:
790 Jointly Inferring Demography and Purifying Selection. *Genetics* **215**: 173-192.
791 Jones FC, Grabherr MG, Chan YF, Russell P, Mauceli E, Johnson J, Swofford R, Pirun M, Zody
792 MC, White S et al. 2012. The genomic basis of adaptive evolution in threespine
793 sticklebacks. *Nature* **484**: 55-61.
794 Kawecki TJ, Lenski RE, Ebert D, Hollis B, Olivieri I, Whitlock MC. 2012. Experimental
795 evolution. *Trends in ecology & evolution* **27**: 547-560.
796 Kellermann V, van Heerwaarden B, Sgro CM, Hoffmann AA. 2009. Fundamental evolutionary
797 limits in ecological traits drive *Drosophila* species distributions. *Science* **325**: 1244-1246.
798 Kelly JK, Hughes KA. 2019. Pervasive Linked Selection and Intermediate-Frequency Alleles
799 Are Implicated in an Evolve-and-Resequencing Experiment of *Drosophila simulans*.
800 *Genetics* **211**: 943-961.
801 Kemppainen P, Li Z, Rastas P, Löytynoja A, Fang B, Guo B, Shikano T, Yang J, Merilä J. 2020.
802 Genetic population structure constrains local adaptation and probability of parallel
803 evolution in sticklebacks. *bioRxiv*.
804 Kerdaffrec E, Filiault DL, Korte A, Sasaki E, Nizhynska V, Seren U, Nordborg M. 2016.
805 Multiple alleles at a single locus control seed dormancy in Swedish Arabidopsis. *Elife* **5**.
806 King EG, Merkes CM, McNeil CL, Hoofer SR, Sen S, Broman KW, Long AD, Macdonald SJ.
807 2012. Genetic dissection of a model complex trait using the Drosophila Synthetic
808 Population Resource. *Genome Res* **22**: 1558-1566.

809 Kofler R, Langmüller AM, Nouhaud P, Otte KA, Schlötterer C. 2016. Suitability of Different
810 Mapping Algorithms for Genome-wide Polymorphism Scans with Pool-Seq Data. *G3*
811 doi:10.1534/g3.116.034488.
812 Kofler R, Pandey RV, Schlötterer C. 2011. PoPoolation2: identifying differentiation between
813 populations using sequencing of pooled DNA samples (Pool-Seq). *Bioinformatics* **27**:
814 3435-3436.
815 Kopp M, Matuszewski S. 2014. Rapid evolution of quantitative traits: theoretical perspectives.
816 *Evol Appl* **7**: 169-191.
817 Langley CH, Tobari YN, Kojima KI. 1974. Linkage disequilibrium in natural populations of
818 Drosophila melanogaster. *Genetics* **78**: 921-936.
819 Langmead B, Salzberg SL. 2012. Fast gapped-read alignment with Bowtie 2. *Nature methods* **9**:
820 357-359.
821 Langmüller AM, Nolte V, Galagedara R, Poupardin R, Dolezal M, Lečić S, S. S. 2020. Fitness
822 effects for Ace insecticide resistance mutations are determined by ambient temperature.
823 *submitted*.
824 Lee KM, Coop G. 2017. Distinguishing Among Modes of Convergent Adaptation Using
825 Population Genomic Data. *Genetics* **207**: 1591-1619.
826 Li H, Durbin R. 2010. Fast and accurate long-read alignment with Burrows-Wheeler transform.
827 *Bioinformatics* **26**: 589-595.
828 Li H, Handsaker B, Wysoker A, Fennell T, Ruan J, Homer N, Marth G, Abecasis G, Durbin R,
829 Genome Project Data Processing S. 2009. The Sequence Alignment/Map format and
830 SAMtools. *Bioinformatics* **25**: 2078-2079.
831 Li J, Li H, Jakobsson M, Li S, Sjodin P, Lascoux M. 2012. Joint analysis of demography and
832 selection in population genetics: where do we stand and where could we go? *Mol Ecol*
833 **21**: 28-44.
834 Li YR, Keating BJ. 2014. Trans-ethnic genome-wide association studies: advantages and
835 challenges of mapping in diverse populations. *Genome Med* **6**: 91.
836 Lohmueller KE. 2014. The impact of population demography and selection on the genetic
837 architecture of complex traits. *PLoS Genet* **10**: e1004379.
838 Mallard F, Nolte V, Tobler R, Kapun M, Schlötterer C. 2018. A simple genetic basis of
839 adaptation to a novel thermal environment results in complex metabolic rewiring in
840 *Drosophila*. *Genome biology* **19**: 119.
841 Mancuso N, Rohland N, Rand KA, Tandon A, Allen A, Quinque D, Mallick S, Li H, Stram A,
842 Sheng X et al. 2016. The contribution of rare variation to prostate cancer heritability. *Nat*
843 *Genet* **48**: 30-35.
844 McCarthy MI, Abecasis GR, Cardon LR, Goldstein DB, Little J, Ioannidis JP, Hirschhorn JN.
845 2008. Genome-wide association studies for complex traits: consensus, uncertainty and
846 challenges. *Nat Rev Genet* **9**: 356-369.
847 Michalak P, Kang L, Schou MF, Garner HR, Loeschcke V. 2019. Genomic signatures of
848 experimental adaptive radiation in *Drosophila*. *Molecular ecology* **28**: 600-614.
849 Morgan TJ, Mackay TF. 2006. Quantitative trait loci for thermotolerance phenotypes in
850 *Drosophila melanogaste*r. *Heredity* **96**: 232-242.
851 Novocraft. 2014. NovoAlign. doi:http://www.novocraft.com/products/novoalign/.

852 Nuzhdin SV, Turner TL. 2013. Promises and limitations of hitchhiking mapping. *Current*
853 *opinion in genetics & development* **23**: 694-699.
854 Otte KA, Schlötterer C. 2017. Polymorphism-aware protein databases - a prerequisite for an
855 unbiased proteomic analysis of natural populations. *Molecular ecology resources*
856 doi:10.1111/1755-0998.12656.
857 Otte KA, Schlötterer C. 2019. A generalised approach to detect selected haplotype blocks in
858 Evolve and Resequence experiments. *bioRxiv*.
859 Palmieri N, Nolte V, Chen J, Schlötterer C. 2015. Genome assembly and annotation of a
860 *Drosophila simulans* strain from Madagascar. *Molecular ecology resources* **15**: 372-381.
861 Pavlidis P, Alachiotis N. 2017. A survey of methods and tools to detect recent and strong
862 positive selection. *J Biol Res (Thessalon)* **24**: 7.
863 Petavy G, David JR, Gibert P, Moreteau B. 2001. Viability and rate of development at different
864 temperatures in Drosophila: a comparison of constant and alternating thermal regimes. *J*
865 *Therm Biol* **26**: 29-39.
866 Pritchard JK, Pickrell JK, Coop G. 2010. The genetics of human adaptation: hard sweeps, soft
867 sweeps, and polygenic adaptation. *Current biology : CB* **20**: R208-215.
868 R Core Team. 2019. R: A Language and Environment for Statistical Computing. R Foundation
869 for Statistical Computing, Vienna, Austria (http://www.r-project.org/index.html).
870 Rako L, Blacket MJ, McKechnie SW, Hoffmann AA. 2007. Candidate genes and thermal
871 phenotypes: identifying ecologically important genetic variation for thermotolerance in
872 the Australian Drosophila melanogaster cline. *Molecular ecology* **16**: 2948-2957.
873 Reid NM, Proestou DA, Clark BW, Warren WC, Colbourne JK, Shaw JR, Karchner SI, Hahn
874 ME, Nacci D, Oleksiak MF et al. 2016. The genomic landscape of rapid repeated
875 evolutionary adaptation to toxic pollution in wild fish. *Science* **354**: 1305-1308.
876 Roesti M, Gavrilets S, Hendry AP, Salzburger W, Berner D. 2014. The genomic signature of
877 parallel adaptation from shared genetic variation. *Mol Ecol* **23**: 3944-3956.
878 Sachdeva H, Barton NH. 2018. Introgression of a Block of Genome Under Infinitesimal
879 Selection. *Genetics* **209**: 1279-1303.
880 Schlötterer C, Tobler R, Kofler R, Nolte V. 2014. Sequencing pools of individuals - mining
881 genome-wide polymorphism data without big funding. *Nature reviews Genetics* **15**: 749-
882 763.
883 Seabra SG, Fragata I, Antunes MA, Faria GS, Santos MA, Sousa VC, Simoes P, Matos M. 2018.
884 Different Genomic Changes Underlie Adaptive Evolution in Populations of Contrasting
885 History. *Mol Biol Evol* **35**: 549-563.
886 Sella G, Barton NH. 2019. Thinking About the Evolution of Complex Traits in the Era of
887 Genome-Wide Association Studies. *Annu Rev Genomics Hum Genet* **20**: 461-493.
888 Shahandeh MP, Turner TL. 2020. The complex genetic architecture of male mate choice
889 evolution between Drosophila species. *Heredity (Edinb)* **124**: 737-750.
890 Shi H, Kichaev G, Pasaniuc B. 2016. Contrasting the Genetic Architecture of 30 Complex Traits
891 from Summary Association Data. *Am J Hum Genet* **99**: 139-153.
892 Simons YB, Turchin MC, Pritchard JK, Sella G. 2014. The deleterious mutation load is
893 insensitive to recent population history. *Nat Genet* **46**: 220-224.

894 Smit AFA, Hubley R, Green P. 2015. RepeatMasker Open-4.0 (2013-2015)
895 (http://www.repeatmasker.org/).
896 Spitzer K, Pelizzola M, Futschik A. 2020. Modifying the Chi-square and the CMH test for
897 population genetic inference: Adapting to overdispersion. *Ann Appl Stat* **14**: 202-220.
898 Stajich JE, Hahn MW. 2005. Disentangling the effects of demography and selection in human
899 history. *Mol Biol Evol* **22**: 63-73.
900 Stam LF, Laurie CC. 1996. Molecular dissection of a major gene effect on a quantitative trait:
901 the level of alcohol dehydrogenase expression in Drosophila melanogaster. *Genetics* **144**:
902 1559-1564.
903 Storz JF. 2005. Using genome scans of DNA polymorphism to infer adaptive population
904 divergence. *Molecular ecology* **14**: 671-688.
905 Tajima F. 1989. Statistical method for testing the neutral mutation hypothesis by DNA
906 polymorphism. *Genetics* **123**: 585-595.
907 Takata R, Takahashi A, Fujita M, Momozawa Y, Saunders EJ, Yamada H, Maejima K, Nakano
908 K, Nishida Y, Hishida A et al. 2019. 12 new susceptibility loci for prostate cancer
909 identified by genome-wide association study in Japanese population. *Nat Commun* **10**:
910 4422.
911 Taus T, Futschik A, Schlötterer C. 2017. Quantifying Selection with Pool-Seq Time Series Data.
912 *Molecular biology and evolution* **34**: 3023-3034.
913 Thornton KR. 2019. Polygenic Adaptation to an Environmental Shift: Temporal Dynamics of
914 Variation Under Gaussian Stabilizing Selection and Additive Effects on a Single Trait.
915 *Genetics* doi:10.1534/genetics.119.302662.
916 Tobler R, Franssen SU, Kofler R, Orozco-Terwengel P, Nolte V, Hermisson J, Schlötterer C.
917 2014. Massive habitat-specific genomic response in *D. melanogaster* populations during
918 experimental evolution in hot and cold environments. *Molecular biology and evolution*
919 **31**: 364-375.
920 Tobler R, Nolte V, Schlotterer C. 2017. High rate of translocation-based gene birth on the
921 Drosophila Y chromosome. *Proceedings of the National Academy of Sciences of the*
922 *United States of America* **114**: 11721-11726.
923 Turner TL, Bourne EC, Von Wettberg EJ, Hu TT, Nuzhdin SV. 2010. Population resequencing
924 reveals local adaptation of *Arabidopsis lyrata* to serpentine soils. *Nature genetics* **42**:
925 260-263.
926 Visscher PM, Macgregor S, Benyamin B, Zhu G, Gordon S, Medland S, Hill WG, Hottenga JJ,
927 Willemsen G, Boomsma DI et al. 2007. Genome partitioning of genetic variation for
928 height from 11,214 sibling pairs. *Am J Hum Genet* **81**: 1104-1110.
929 Vitti JJ, Grossman SR, Sabeti PC. 2013. Detecting natural selection in genomic data. *Annual*
930 *review of genetics* **47**: 97-120.
931 Vlachos C, Kofler R. 2018. MimicrEE2: Genome-wide forward simulations of Evolve and
932 Resequencing studies. *PLoS computational biology* **14**: e1006413.
933 Wojcik GL, Graff M, Nishimura KK, Tao R, Haessler J, Gignoux CR, Highland HM, Patel YM,
934 Sorokin EP, Avery CL et al. 2019. Genetic analyses of diverse populations improves
935 discovery for complex traits. *Nature* **570**: 514-518.

936 Wu Y, Waite LL, Jackson AU, Sheu WH, Buyske S, Absher D, Arnett DK, Boerwinkle E,
937 Bonnycastle LL, Carty CL et al. 2013. Trans-ethnic fine-mapping of lipid loci identifies
938 population-specific signals and allelic heterogeneity that increases the trait variance
939 explained. *PLoS Genet* **9**: e1003379.
940 Xu S. 2003. Theoretical basis of the Beavis effect. *Genetics* **165**: 2259-2268.
941 Yang J, Manolio TA, Pasquale LR, Boerwinkle E, Caporaso N, Cunningham JM, de Andrade M,
942 Feenstra B, Feingold E, Hayes MG et al. 2011. Genome partitioning of genetic variation
943 for complex traits using common SNPs. *Nat Genet* **43**: 519-525.
944 Yeaman S, Whitlock MC. 2011. The genetic architecture of adaptation under migration-selection
945 balance. *Evolution; international journal of organic evolution* **65**: 1897-1911.
946 Zan Y, Carlborg O. 2019. A Polygenic Genetic Architecture of Flowering Time in the
947 Worldwide Arabidopsis thaliana Population. *Mol Biol Evol* **36**: 141-154.
948 Zan Y, Sheng Z, Lillie M, Ronnegard L, Honaker CF, Siegel PB, Carlborg O. 2017. Artificial
949 Selection Response due to Polygenic Adaptation from a Multilocus, Multiallelic Genetic
950 Architecture. *Molecular biology and evolution* **34**: 2678-2689.
951 Zeng J, de Vlaming R, Wu Y, Robinson MR, Lloyd-Jones LR, Yengo L, Yap CX, Xue A,
952 Sidorenko J, McRae AF et al. 2018. Signatures of negative selection in the genetic
953 architecture of human complex traits. *Nature genetics* **50**: 746-753.
954 Zhang XS, Hill WG. 2005. Predictions of patterns of response to artificial selection in lines
955 derived from natural populations. *Genetics* **169**: 411-425.